JAAS FULL PAPER
www.rsc.org/jaas

Calculation of the gas flow and its effect on the plasma characteristics for a modified Grimm-type glow discharge cell†

Annemie Bogaerts,* Andriy Okhrimovskyy and Renaat Gijbels

University of Antwerp, Department of Chemistry, Universiteitsplein 1, B-2610 Wilrijk-Antwerp, Belgium. E-mail: annemie.bogaerts@ua.ac.be

Received 21st January 2002, Accepted 27th February 2002
First published as an Advance Article on the web 26th March 2002

Based on a computational fluid dynamics model, the argon gas flow in a Grimm-type glow discharge cell was calculated. Its effect on the plasma characteristics was investigated by adding convection as an additional transport mechanism of the plasma species as well as diffusion and migration. The Ar gas convection velocity, at an inlet gas flow rate of 100 sccm, was calculated to be of the order of a few tens to a hundred m s^{-1}, increasing to a few hundred m s^{-1} at the gas inlet and outlet positions. The Ar gas atom density was found to be distributed slightly non-uniformly in the plasma. The calculated Ar gas flow appeared to have only a minor effect on the density distributions of the plasma species, but their fluxes were significantly affected. It appears that, under the conditions investigated, convection is the dominant transport mechanism in the negative glow for all plasma species, except for the electrons. Therefore, the calculated ion fluxes at the exit towards the mass spectrometer appear to increase with gas flow rate, which is in accordance with experimental observations.

1 Introduction

In recent years, we have developed a comprehensive modeling network for analytical glow discharges in dc, rf and pulsed operation mode (*e.g.*, refs. 1–3). A number of Monte Carlo, fluid and collisional-radiative models were developed for the various plasma species, *i.e.*, electrons, Ar^+ ions, fast Ar atoms, Ar atoms in various excited levels, sputtered Cu atoms and the corresponding ions, both in the ground state and in various excited levels. The behavior of the Ar gas atoms was generally not calculated; it was simply assumed that there was no major gas flow and that the Ar gas atoms were at thermal velocities uniformly distributed throughout the discharge. It should, however, be mentioned that we have also developed a model to calculate gas heating.[4]

On the other hand, there is in reality always a certain gas flow and, especially in recent developments of glow discharge mass spectrometry (GDMS), a considerable gas flow is produced in the discharge to increase the ion transport towards the mass spectrometer.[5] Therefore, we wish to extend our modeling network by including the effect of gas flow in the models. The gas flow itself was calculated by a computational fluid dynamics (CFD) program, and this result was used as input into our plasma models in order to calculate the transport of the plasma species, not only by diffusion and migration, but also by convection. In the following, both the CFD program and the incorporation of convection in the plasma models will be briefly outlined, and the results of this coupling will be presented and discussed.

2 Description of the model

2.1 CFD program to calculate the gas flow

The computational fluid dynamics (CFD) program, which was used to calculate the gas flow in the glow discharge cell, is a commercial code called "FLUENT" (version 5.5.14 for IRIX64).[6] It is based on the balance equations for mass, impulse and energy. For our calculations, we assumed a laminar gas flow. It is applied here to a modified Grimm-type glow discharge cell, which is under investigation as an ion source for GDMS.[5] A schematic picture of the cell geometry[5] is presented in Fig. 1. Although the actual cell geometry is not fully axially symmetrical with respect to gas inlet and outlet, we used the CFD program in only two dimensions (based on an axisymmetric approximation) in order to avoid too long computation times and because it is coupled to the two-dimensional plasma models (see below). There is one gas inlet position and two gas outlet positions, as is shown in Fig. 1. We typically assumed an inlet gas flow rate of 100 sccm, whereas the outlet gas flow rates are determined by the background pressures outside the glow discharge cell. The latter are assumed to be 3.4 Pa at the outlet towards the mass spectrometer and 73 Pa at the additional outlet, indicated in Fig. 1, which is based on measured data.[5] It is worth mentioning that this additional outlet is meant to avoid excessive gas flow towards the mass spectrometer and subsequent overloading of the vacuum system.

2.2 Incorporation of the gas flow into the plasma models

As mentioned above, we have previously developed a hybrid modeling network[4,7–15] consisting of a number of Monte Carlo, fluid and collisional-radiative models for the various species present in the plasma, as is illustrated in Table 1. In this

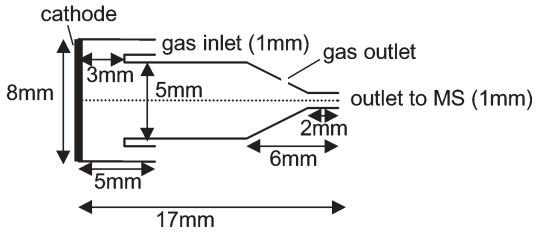

Fig. 1 Schematic diagram of the cell geometry under investigation in this work, illustrating the position of the cathode, and the gas inlet and outlet positions. This cell geometry is a modified Grimm-type cell, which is currently under investigation to be used as an ion source for glow discharge mass spectrometry.[5]

†Presented at the 2002 Winter Conference on Plasma Spectrochemistry, Scottsdale, AZ, USA, January 6–12, 2002.

 DOI: 10.1039/b200746k

Table 1 Overview of the different species assumed to be present in the plasma, and the models used to describe their behavior. References where more information can be found about the individual models are also cited

Species	Model	Ref.
Ar gas atoms	Previous work: no model (thermal + uniform), or gas heating by heat transfer equation	4
	New: gas flow by CFD program	—
Fast electrons	Monte Carlo model	7,8
Slow electrons	Fluid model	8,9
Ar^+ ions	Fluid model	8,9
Fast Ar^+ ions in the CDS	Monte Carlo model	7,10
Fast Ar atoms in the CDS	Monte Carlo model	7,10
Ar atoms in 64 excited levels	Collisional-radiative model	11
Sputtering of Cu	Formula for sputtering yield	12
Thermalization of Cu atoms	Monte Carlo model	13
Cu atoms in 8 different levels (including ground state)	Collisional-radiative model	14
Cu^+ ions in 7 different levels (including ground state)	Collisional-radiative model	14
Fast Cu^+ ions in the CDS	Monte Carlo model	15

modeling network, it was assumed that (i) the Ar gas atoms were at thermal energies and uniformly distributed throughout the discharge (although a model was also developed to calculate gas heating of the Ar gas, but no gas flow) and (ii) the transport of the plasma species was dictated only by migration (for the charged plasma species) and diffusion, and transport by convection was neglected.

In the improved plasma modeling network presented in this paper, the effect of the gas flow is taken into account (i) by assuming a non-uniform Ar gas atom density distribution and (ii) by adding convection as an additional transport mechanism for the plasma species. We will focus here only on these improvements, because other details about the models have been previously published.[1,4,7–15]

The non-uniform Ar gas atom density comes into play when determining the occurrence of collisions of the plasma species with Ar gas atoms in the Monte Carlo models. This is only a minor modification to the previous models and was actually already carried out when calculating gas heating, which also yielded a non-uniform distribution of the Ar gas density.[4]

The second modification was, however, more important, *i.e.*, the addition of a convection term in the transport equations of the plasma species in the fluid and collisional-radiative models. This gives rise to the following general transport equation for a particular species "k":

$$\boldsymbol{J}_k = -D_k \nabla n_k \ (\pm \mu_k n_k \boldsymbol{E}) + n_k \boldsymbol{U}_{conv}$$

Here, $\boldsymbol{J}$ and n are the species flux (vector notation) and density, D and μ are the diffusion coefficient and mobility of species k, $\boldsymbol{E}$ is the electric field, and $\boldsymbol{U}_{conv}$ is the convection velocity as a result of the gas flow. The first term denotes transport by diffusion (∇n_k stands for the density gradient). The second term stands for migration as a result of the electric field and must only be considered for charged plasma species (hence the brackets). The plus sign is used for positive ions, whereas the minus sign applies to electrons. The last term of the transport equation represents convection; hence, the flux by convection is equal to the convection velocity of the Ar gas flow multiplied by the density of species k.

All models for the different plasma species are solved iteratively, until convergence is reached, as explained in previous work.[1] In principle, there could be a coupling-back from the plasma models towards the CFD program, *i.e.*, to calculate the gas heating because it also determines the background Ar gas density.[4] However, at this moment this has not yet been implemented in the CFD code, and the purpose of the present work is to show the effect of the gas flow on the density and flux of the plasma species, for which the gas heating is of minor importance. Nevertheless, it might be the subject of a future investigation.

Finally, it is worth mentioning that this way of coupling a CFD code with the plasma models is only one approach to describing the effect of the gas flow in a glow discharge cell. An alternative would be to combine the plasma species reactions and flow dynamics into one model, as is described in the software Plasimo,[16,17] albeit for different kinds of plasmas.

3 Results and discussion

3.1 Results of the CFD program

The calculations are performed for the cell geometry presented in Fig. 1. The background pressures at the outlets are given above and the inlet gas flow is assumed to be 100 sccm, unless mentioned otherwise. The applied discharge voltage is 700 V and the resulting current was calculated to be 60 mA.

Fig. 2 shows the axial (a) and radial (b) convection velocities of the Ar gas in the two-dimensional cell geometry, as calculated with the CFD program. It should be mentioned that the gas velocity is zero at the cell walls (given as boundary condition in the model). However, due to rather strong gradients, this is not really visible in Fig. 2. The axial velocity

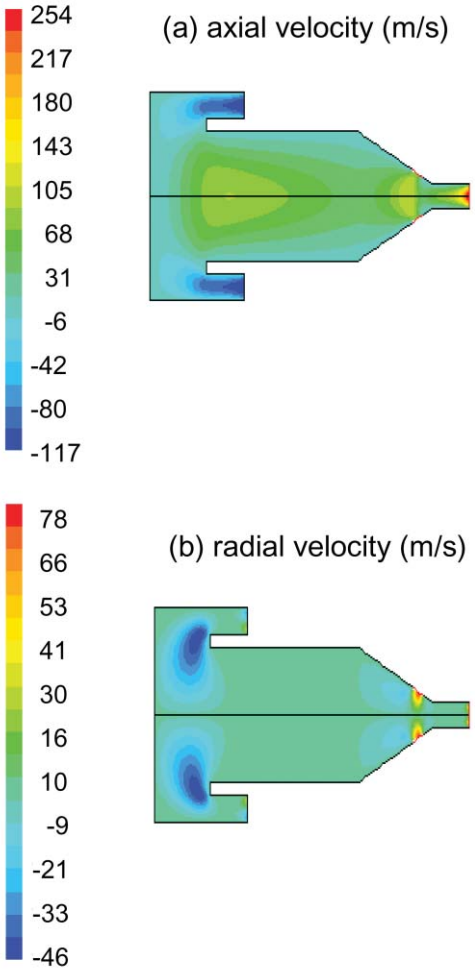

Fig. 2 Axial (a) and radial (b) convection velocities of the Ar gas in the two-dimensional cell geometry, as calculated with the computational fluid dynamics code, for a gas inlet flow rate of 100 sccm, and background pressures at the gas outlet positions of 3.4 Pa and 73 Pa (at the outlet towards the mass spectrometer and the additional outlet, respectively).

is highly negative (*i.e.*, directed towards the left) at the gas inlet position, but in most of the cell geometry it is positive, *i.e.*, directed towards the right (away from the cathode towards the entrance of the mass spectrometer). It becomes especially high (several 100 m s^{-1}) at the outlet to the mass spectrometer. In general, the axial velocity is calculated to be of the order of a few 10s to 100 m s^{-1}, as is apparent from the color scale in Fig. 2(a). Finally, it is also apparent that the axial velocity is highest at the cell axis and drops gradually towards the sidewalls of the cell.

The radial convection velocity is characterized by somewhat lower values than the axial velocity, as is clear from Fig. 2(b). It is highly negative, *i.e.*, directed towards the cell axis, near the gas inlet in front of the cathode and highly positive, *i.e.*, directed towards the sidewalls of the cell, at the additional gas outlet. In the main part of the discharge the radial convection velocity is, however, very small (between +10 and −10 m s^{-1}). Hence, from the combination of axial and radial convection velocities, the trajectory of the Ar gas flow can be interpreted as follows: the Ar gas enters at the gas inlet and moves with a high velocity in the direction of the cathode; then it turns and moves away from the cathode through the whole discharge cell until it is accelerated at both gas outlet positions.

The two-dimensional Ar gas atom density distribution, as calculated with the CFD program, is illustrated in Fig. 3. The density is highest near the gas inlet and lowest at both gas outlet positions, as expected. In the main part of the discharge cell, the Ar gas atom density was calculated to be slightly non-uniformly distributed, with values between 4×10^{16} and 5×10^{16} cm^{-3}. These values are realistic for the conditions under investigation, because they correspond to an overall gas pressure and temperature of about 3.5–4 Torr and 800 K when calculated with the ideal gas law ($n = p/kT$). It should, however, be mentioned that gas heating as a result of power input into the Ar gas by collisions of the other plasma species is not yet taken into account in the CFD program. Because the gas heating is at maximum near the cathode, this would lead to a slightly lower density near the cathode. However, as mentioned above, this somewhat different Ar gas atom density distribution would only slightly affect the number of collisions near the cathode, and would have a negligible effect on the calculated density distributions and fluxes of the plasma species.

3.2 Results of the plasma models

3.2.1 Plasma species densities. The two-dimensional density distributions of the Ar^+ ions, Ar metastable atoms, sputtered Cu atoms and corresponding Cu^+ ions, as calculated with our plasma models, are depicted in Fig. 4(a)–(d). It seems as if the density contour lines do not follow the boundaries of the walls. This is, however, simply because the plot program used to construct Fig. 4 can only handle a rectangular geometry. In the actual model result, however, the species densities are zero (or very low) at the cell walls, as is imposed as boundary conditions in the model.

The Ar^+ ion density (Fig. 4(a)) reaches a maximum at about 1–2 mm from the cathode, *i.e.*, in the beginning of the negative

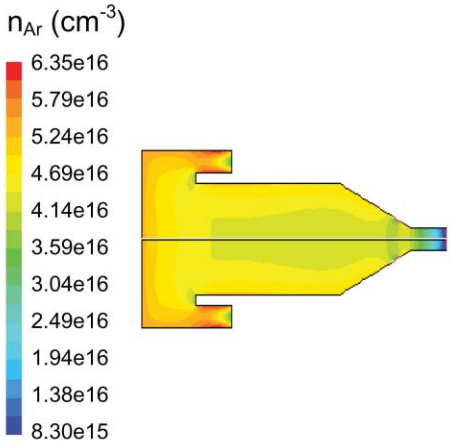

Fig. 3 Two-dimensional Ar gas atom density distribution, as calculated with the computational fluid dynamics code, for the same cell geometry and gas flow conditions as in Fig. 2.

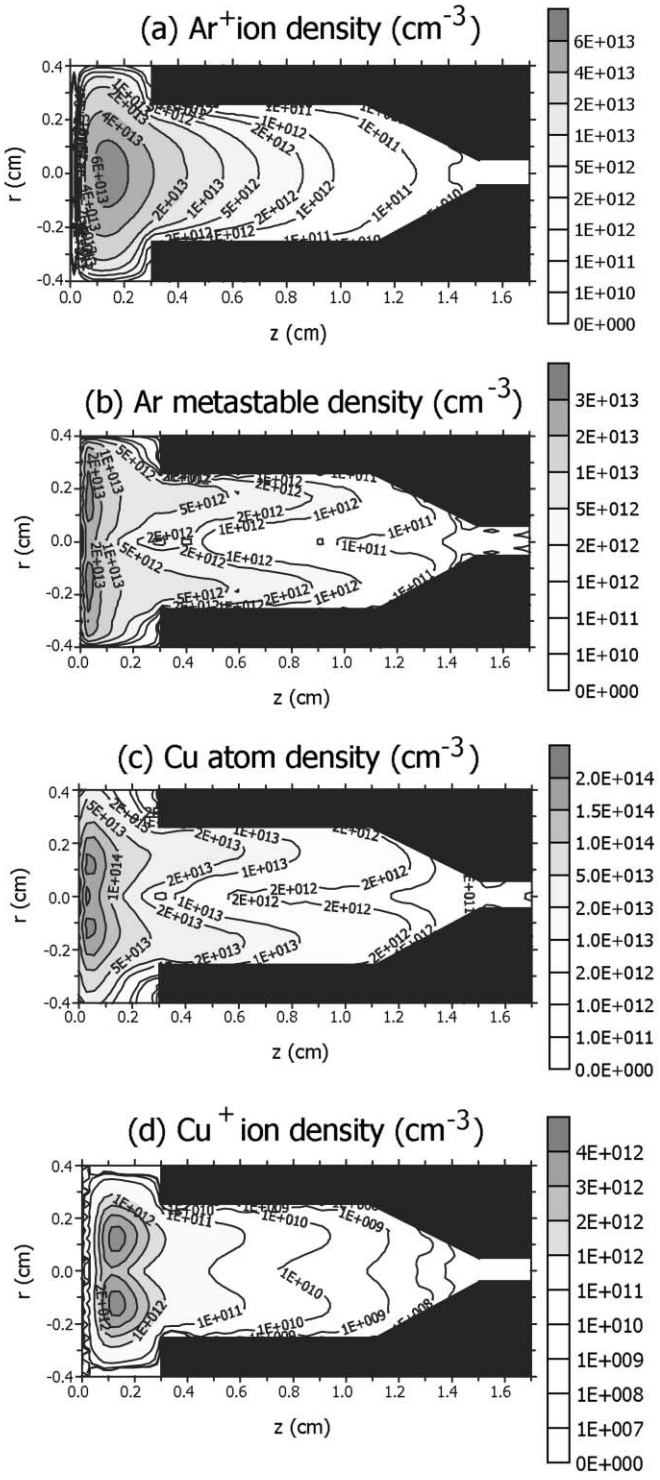

Fig. 4 Two-dimensional density distributions of the Ar^+ ions (a), Ar metastable atoms (b), sputtered Cu atoms (c) and Cu^+ ions (d), as calculated with our plasma models, at 700 V discharge voltage and 60 mA electrical current, and for the same cell geometry and gas flow conditions as in Fig. 2.

glow (NG), and drops over several orders of magnitude as a function of distance from the cathode towards the end of the cell. The calculated electron density is characterized by the same profile, except that it is zero in the cathode dark space (CDS), giving rise there to a positive space charge and hence a strong electric field.

The calculated Ar metastable atom density (Fig. 4(b)) is characterized by a pronounced maximum near the cathode, which drops again as a function of distance from the cathode. Moreover, the Ar metastable density shows a local dip at the cell axis, which is attributed to the higher axial convection velocity at the cell axis (see above). Indeed, the particle flux is equal to the product of density and velocity. Hence, for a constant flux, a higher velocity results in a lower local density, because the particles have left a certain position more rapidly. In reality, the situation is somewhat more complicated, because the flux will not be constant in space. However, a higher velocity typically results in a lower density.

A similar behavior is observed for the calculated sputtered Cu atom density (see Fig. 4(c)). It also reaches a maximum near the cathode, drops towards the end of the cell as a function of distance from the cathode, and is characterized by a low-density wedge at the cell axis, due to the slightly higher axial convection velocity.

The corresponding calculated two-dimensional Cu^+ ion density is depicted in Fig. 4(d). Its profile resembles that of the Ar^+ ion density, with a maximum at about 1–2 mm from the cathode and again a drop as a function of distance from the cathode. The value of the maximum is only about an order of magnitude lower than the maximum Ar^+ ion density, but the Cu^+ ion density drops somewhat more rapidly as a function of distance from the cathode. The reason is that the Ar^+ ions are created from the Ar gas atoms, which are at least more or less uniformly distributed throughout the discharge (see Fig. 3), and the drop in Ar^+ ion density is due to a drop in the ionization efficiency as a function of distance from the cathode. The Cu^+ ions, on the other hand, are created by ionization from the Cu atoms, which are characterized by a decreasing density in the axial direction (see Fig. 4(c)). Hence, the faster drop in Cu^+ ion density is due to both the drop in Cu atom density and the drop in ionization efficiency.

We have also calculated the densities of the above plasma species when no gas flow is present in the discharge. It appears that the calculated density profiles are not greatly affected by the gas flow. For the Ar^+ ions and electrons, no difference at all was observed. For the Ar metastable atoms and sputtered Cu atoms, the calculated density profiles without gas flow were not characterized by a local dip at the cell axis, which confirms that the latter is due to the higher convection velocity at the cell axis. The largest difference was observed for the Cu^+ ion density, which was found to fall even more rapidly as a function of distance from the cathode in the absence of gas flow, *i.e.*, about one order of magnitude faster drop compared to an inlet gas flow rate of 100 sccm.

3.2.2 Fluxes of the plasma species. Because the calculated densities plunge as a function of distance from the cathode, it is expected that the fluxes of ions entering the mass spectrometer (which is located at the end of the discharge cell) are rather low, especially when the cell is rather long. The Grimm-type cell under investigation to be used as an ion source for mass spectrometry (schematic presented in Fig. 1)[5] is already considerably shorter than the typical Grimm-type cells used for optical emission spectrometry[18] in order to have sufficient ions entering the mass spectrometer. However, by forcing a considerable gas flow through the discharge cell, the transport of the ions and of the plasma species in general to the end of the cell will be promoted, which is the idea behind the new ion source development.[5] To check this idea, we calculated the fluxes of the plasma species for different gas inlet flow rates and compared them to a zero gas flow rate. Moreover, we also investigated the relative roles of the various transport mechanisms, *i.e.*, diffusion, migration and convection, for the various plasma species.

Fig. 5 illustrates the calculated fluxes of the Ar^+ ions (a), Ar metastable atoms (b), sputtered Cu atoms (c) and Cu^+ ions (d) as a function of distance from the cathode, as well as the individual contributions by diffusion, migration (for the ions) and convection. The left-hand figures are on a linear scale. Because the flux drops off considerably as a function of distance from the cathode (as a result of the drop in the densities and in the density gradients, see above) and because we are especially interested in the transport towards the mass spectrometer (at least for the ions), we have also presented the same data on a semi-log plot in the right-hand figures (hence, only positive values are plotted) in order to visualize the contributions of the different transport mechanisms towards the end of the cell.

It is clear from Fig. 5(a) that the flux of Ar^+ ions is extremely negative towards the cathode, as a result of migration in the strong electric field in the CDS (see left part: linear scale). However, the right part (logarithmic scale) shows that, in the NG, convection is the dominant transport mechanism towards the end of the cell, with relative contributions calculated to be of the order of 50–70% (the rest is mainly due to migration) and increasing even up to 90% at the end of the cell. The Ar^+ ion flux appears to increase slightly at the end of the cell, which is attributed to the higher axial convection velocity at the gas outlet position towards the mass spectrometer (see Fig. 2(a)).

The flux of Ar metastable atoms (see Fig. 5(b)) is also extremely negative, *i.e.*, directed towards the cathode, near the cathode (see left part: linear scale), which is attributed to diffusion. Indeed, the Ar metastable atom density reaches a pronounced maximum near the cathode and the large density gradient, which is the result of this, gives rise to a large diffusion flux. However, after the maximum Ar metastable atom density, the transport of Ar metastable atoms is directed towards the end of the cell and is almost exclusively (90–100%) due to convection, as appears from the right-hand of Fig. 5(b) (logarithmic scale).

A similar behavior is observed for the sputtered Cu atoms, as appears from Fig. 5(c), which is to be expected because the density profiles of Ar metastable atoms and sputtered Cu atoms were also found to be very similar (see Fig. 4(b) and (c)). Hence, near the cathode, the Cu atom flux is again very negative, *i.e.*, directed towards the cathode, due to diffusion processes as a result of the large density gradient (see left part: linear scale), whereas convection is again the dominant transport mechanism in the rest of the plasma (see right part: logarithmic scale), with a calculated relative contribution of 80–95%.

Finally, the flux of Cu^+ ions is illustrated in Fig. 5(d). It again shows a similar behavior to the Ar^+ ions, with a highly negative flux (directed towards the cathode) in the CDS due to migration in the strong electric field (see left part: linear scale). In the NG, the transport is due to both convection and migration, and diffusion is of minor importance (see right part: logarithmic scale). The relative contribution of convection was calculated to be of the order of 40–60%, increasing up to 70% at the end of the cell, *i.e.*, near the outlet to the mass spectrometer.

It is worthwhile mentioning that we assumed that the ions only enter the mass spectrometer by means of the pressure gradient (and the resulting gas flow), and that we neglected any contribution from the acceleration voltage of the mass spectrometer. In reality, however, an acceleration voltage of about 1 kV is typically applied.[5] This would further increase the ion fluxes entering the mass spectrometer. However, the effect of the acceleration voltage, in absolute terms, would be the same with and without applying a gas flow and, because we are

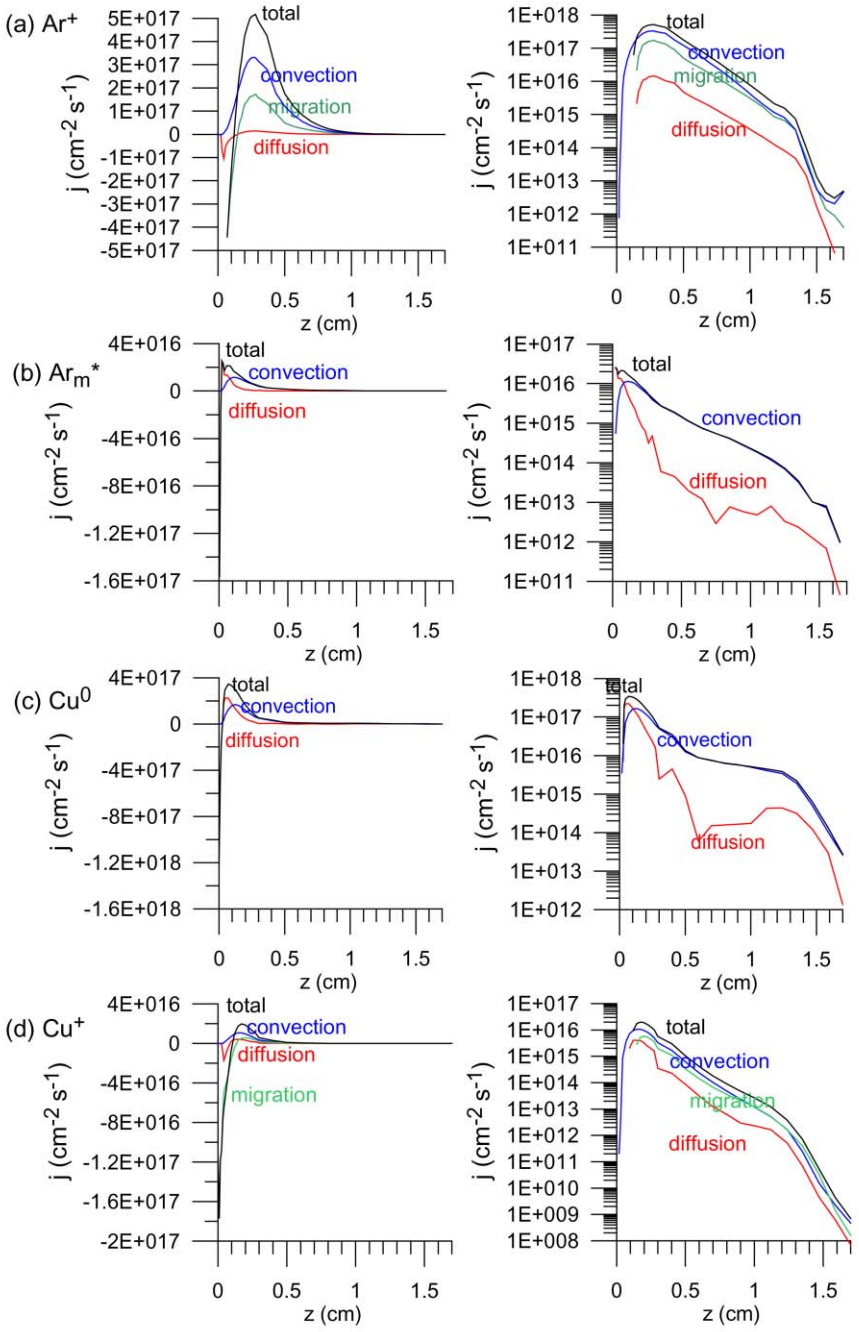

Fig. 5 Calculated fluxes as a function of distance from the cathode, taken at the cell axis, for the Ar^+ ions (a), Ar metastable atoms (b), sputtered Cu atoms (c) and Cu^+ ions (d), under the same conditions as in Fig. 4. The calculated contributions of the different transport mechanisms by diffusion, migration (for the ions) and convection are also illustrated. The figures at the left-hand side are on a linear scale, whereas the figures at the right-hand side are semi-log plots for visualizing the important role of convection in the NG towards the end of the cell.

investigating the effect of the gas flow, this is not of major concern here.

From Fig. 5(a)–(d) it is clear that convection is the most important transport mechanism of the plasma species in the NG and towards the end of the cell. This is true for all plasma species, except for the electrons (not presented here). Indeed, due to their much lower mass, the electrons are characterized by a much higher diffusion coefficient and mobility (several orders of magnitude), so that diffusion and migration are still more important transport mechanisms for the electrons than convection at the typical gas flow rates under study (order of 100 sccm).

To investigate the effect of gas flow, we compared the fluxes of the above plasma species, calculated for an inlet gas flow rate of 100 sccm, with the calculated fluxes without gas flow. The results are presented in Fig. 6(a)–(d) for the Ar^+ ions, Ar metastable atoms, sputtered Cu atoms and Cu^+ ions, respectively. In general, it is found that the fluxes of the plasma species with an inlet gas flow rate of 100 sccm are higher than the calculated fluxes without gas flow, which is to be expected because of the important role of convection, as shown above.

Finally, Fig. 7 shows the calculated fluxes of Ar^+ ions (a) and Cu^+ ions (b) at the entrance of the mass spectrometer as a function of gas flow rate. It is clear that the calculated fluxes increase with gas flow rate, which is again to be expected because a higher gas flow rate means a higher convection velocity and hence a larger contribution of convection as transport mechanism and therefore a higher flux. The increase was found to be more or less linear for the Ar^+ ions, whereas the Cu^+ ions appear to behave in a more complicated way. Indeed, they are the result of the Cu atom density and the efficiency of different ionization mechanisms, *i.e.*, asymmetric

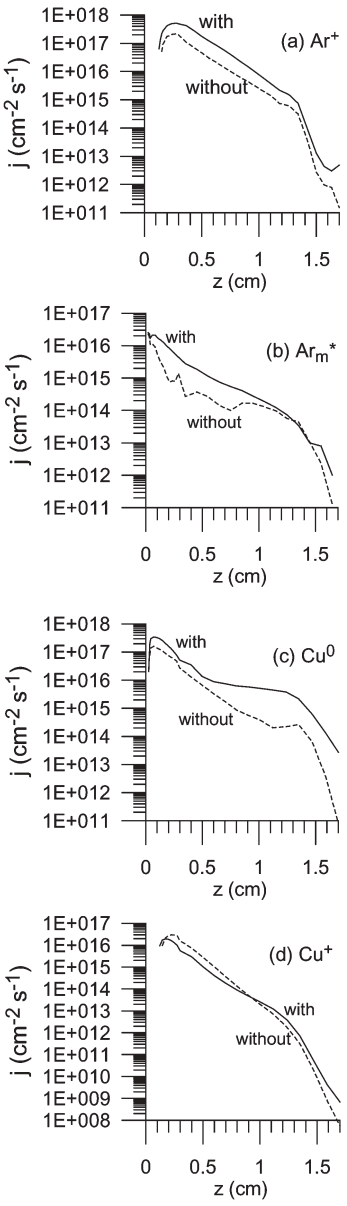

Fig. 6 Calculated fluxes as a function of distance from the cathode, taken at the cell axis, for the Ar^+ ions (a), Ar metastable atoms (b), sputtered Cu atoms (c) and Cu^+ ions (d), for an inlet gas flow rate of 100 sccm (solid lines) and no gas flow (dashed line). The other conditions are the same as in Fig. 4.

charge transfer with Ar^+ ions, electron impact and Penning ionisation. Hence, non-linear effects are not unexpected.

Fig. 7(b) also illustrates experimental data, *i.e.*, the measured Cu^+ ion intensities in the mass spectrometer, as a function of gas flow for the same cell geometry and conditions as assumed in our model.[5] It appears that the measured Cu^+ ion intensities rise somewhat more rapidly with gas flow rate than our calculated values, which is probably due to the complexity of our models and the corresponding uncertainties. Nevertheless, calculated and measured data show at least a similar increasing trend as a function of gas flow rate. For the Ar^+ ion intensities, the experimental data[5] did not reveal an increasing trend as a function of gas flow rate, which is unexpected (in view of our discussions given above) and can probably be attributed to some secondary effects in the experiment (*e.g.*, may be related to the effect of hydrogen, because the ArH^+ ion intensities in the mass spectra appeared to be very high). On the other hand, Tanaka *et al.*[19] investigated the effect of gas flow rate in a Grimm-type ion source on various ion intensities, and reported that all ion signals increased significantly with gas flow rate. The effect was found to be most pronounced for the Ar^+ ions.[19] This suggests that our calculation results are at least qualitatively correct.

4 Conclusion

In order to investigate the effect of the Ar gas flow on the plasma characteristics, we calculated the Ar gas convection velocity with a computational fluid dynamics (CFD) program for a Grimm-type cell geometry, which is currently under investigation to be used as an ion source for mass spectrometry.[5] The output of this CFD program, *i.e.*, the calculated axial and radial convection velocities and the Ar gas atom density distribution, were used as input into the previously developed hybrid modeling network for the glow discharge plasma.[1] Two kinds of modifications had to be applied to our plasma models: (i) the Ar gas atom density is non-uniformly distributed throughout the discharge, which affects the number of collisions as calculated in the Monte Carlo models; and (ii) transport by convection has to be added as an additional term in the transport equations of the plasma species in the fluid and collisional-radiative models.

It was found that the gas flow had only a minor effect on the calculated density distributions of the various plasma species, but the effect on the calculated fluxes was found to be very important (except for the electrons). Indeed, under the conditions in this study, *i.e.*, typical inlet gas flow rate of 100 sccm, convection was found to be the dominant transport mechanism in the NG and towards the end of the cell for all plasma species, except for the electrons. It is therefore not unexpected that the calculated ion fluxes of Ar^+ and Cu^+ ions at the entrance of the mass spectrometer increase with rising gas flow rate. This is at least in qualitative agreement with experimental observations from the literature.[5,19]

Hence, it can be concluded that, because of the efficient

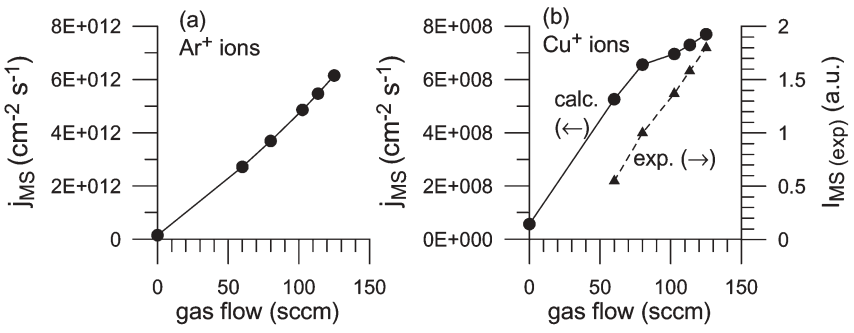

Fig. 7 Calculated fluxes of the Ar^+ (a) and Cu^+ ions (b) at the entrance of the mass spectrometer, as a function of inlet gas flow rate (solid lines). Also presented in Fig. 7(b) are the measured Cu^+ ion intensities in the mass spectrometer[5] for the same conditions as assumed in our model (broken line).

transport mechanism of convection, forcing a considerable gas flow through a glow discharge cell will increase the ion transport to the mass spectrometer, and hence improve the sensitivity of GDMS.

Acknowledgements

A. Bogaerts and A. Okhrimovskyy are indebted to the Flemish Fund for Scientific Research (FWO-Flanders) for financial support. This research is also sponsored by the Federal Services for Scientific, Technical and Cultural Affairs of the Prime Minister's Office (DWTC/SSTC) through IUAP-V. The authors are also very grateful to M. C. M. van de Sanden and Eindhoven University of Technology for the use of the computational fluid dynamics code as well as the computation time, in the framework of a NATO SfP project. Finally, the authors thank R. Dorka and V. Hoffmann (IFW Dresden) for supplying the experimental data (*i.e.*, cell geometry, gas inlet and outlet flows, and Cu^+ ion intensities in the mass spectrometer) and for the many interesting discussions.

References

1 A. Bogaerts and R. Gijbels, *J. Anal. At. Spectrom.*, 1998, **13**, 945.
2 A. Bogaerts and R. Gijbels, *J. Anal. At. Spectrom.*, 2000, **15**, 1191.
3 A. Bogaerts and R. Gijbels, *J. Anal. At. Spectrom.*, 2001, **16**, 239.
4 A. Bogaerts, R. Gijbels and V. V. Serikov, *J. Appl. Phys.*, 2000, **87**, 8334.
5 R. Dorka and V. Hoffmann, personal communication.
6 Fluent Version 5.5.14 (1998) Fluent Inc. (http://www.fluent.com).
7 A. Bogaerts, M. van Straaten and R. Gijbels, *Spectrochim. Acta, Part B*, 1995, **50**, 179.
8 A. Bogaerts, R. Gijbels and W. J. Goedheer, *J. Appl. Phys.*, 1995, **78**, 2233.
9 A. Bogaerts, R. Gijbels and W. J. Goedheer, *Anal. Chem.*, 1996, **68**, 2296.
10 A. Bogaerts and R. Gijbels, *J. Appl. Phys.*, 1995, **78**, 6427.
11 A. Bogaerts, R. Gijbels and J. Vlcek, *J. Appl. Phys.*, 1998, **84**, 121.
12 N. Matsunami, Y. Yamamura, Y. Itikawa, N. Itoh, Y. Kazumata, S. Miyagawa, K. Morita, R. Shimizu and H. Tawara, *At. Data Nucl. Data Tables*, 1984, **31**, 1.
13 A. Bogaerts, M. van Straaten and R. Gijbels, *J. Appl. Phys.*, 1995, **77**, 1868.
14 A. Bogaerts, R. Gijbels and R. J. Carman, *Spectrochim. Acta, Part B*, 1998, **53**, 1679.
15 A. Bogaerts and R. Gijbels, *J. Appl. Phys.*, 1996, **79**, 1279.
16 G. M. Janssen, J. van Dijk, D. A. Benoy, M. A. Tas, K. T. A. L. Burm, W. J. Goedheer, J. A. M. van der Mullen and D. C. Schram, *Plasma Sources Sci. Technol.*, 1999, **8**, 1.
17 G. M. Janssen, PhD Thesis, Eindhoven University of Technology, 2000.
18 W. Grimm, *Spectrochim. Acta, Part B*, 1968, **23**, 443.
19 T. Tanaka, T. Kubota and H. Kawaguchi, *Anal. Sci.*, 1994, **10**, 895.